Title

CHEMICAL STABILITY OF SODIUM BETA""-ALUMINA ELECTROLYTE IN SULFUR/SODIUM POLYSULFIDE MELTS

Authors

Liu, M.
Jonghe, L.C. De

Publication Date

1986-06-01

Lawrence Berkeley Laboratory
UNIVERSITY OF CALIFORNIA

Materials & Molecular Research Division

Submitted to Journal of the Electrochemical Society

CHEMICAL STABILITY OF SODIUM BETA"-ALUMINA ELECTROLYTE IN SULFUR/SODIUM POLYSULFIDE MELTS

M. Liu and L.C. De Jonghe

June 1986

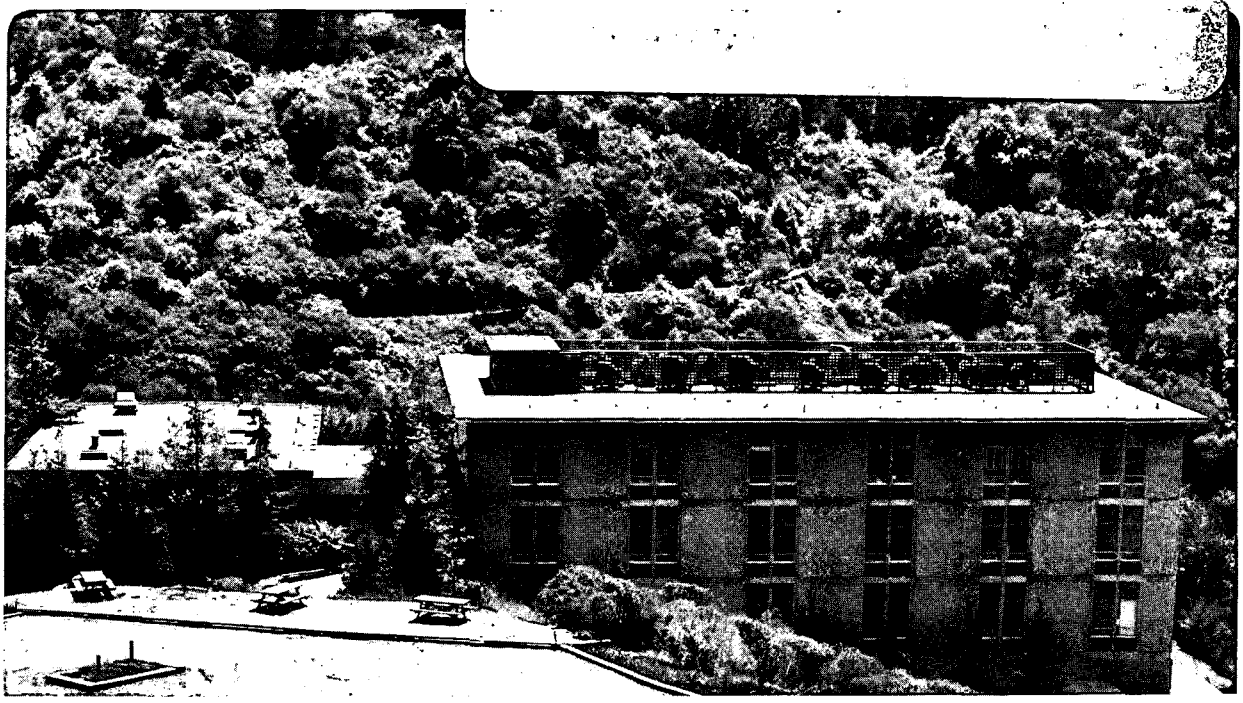

Prepared for the U.S. Department of Energy under Contract DE-AC03-76SF00098

DISCLAIMER

Chemical Stability of Sodium Beta"-Alumina Electrolyte in Sulfur/Sodium Polysulfide Melts

Meilin Liu and L. C. De Jonghe

Materials and Molecular Research Division
Lawrence Berkeley Laboratory
and
Department of Materials Science and Mineral Engineering
University of California, Berkeley
California 94720

ABSTRACT

Immersion of sodium β" alumina electrolyte in sodium polysulfide and pure sulfur melts, at Na/S battery operation temperatures, showed that the electrolyte was chemically attacked by the melts, and that the extent of degradation was affected by a number of factors, including surface morphology and chemistry of the electrolyte, melt composition, impurity contamination, etc. The corrosion reactions mostly initiated and concentrated on defected areas, and were catalyzed by the presence of impurities such as water, moist air, oxygen, etc.. The corrosion power of sodium polysulfide melts increased with the sulfur content in the range of Na_2S_2 to Na_2S_5. The reaction products, formed at the interface, were believed to be Na_2SO_4, $NaAl(SO_4)_2$, $Al_2(SO_4)_3$, $NaHSO_4$, Na_2CO_3 , $NaOH$, etc. Recrystallization of the sulfates occurred on preferred areas after saturation. Corrosion products of transition metals also deposited on the electrolyte surface. As a result, a partly insulating layer was formed on the electrolyte surface during immersion, which was a mixture of sulfates, carbonates, and sulfides of transition metals.

1. Introduction

Degradation of β"-electrolyte is one of the important limitations which determine whether or not Na/S batteries may be useful for energy storage and conversion systems. While there has been considerable effort in establishing the mechanism of degradation of the electrolyte in contact with the negative electrode (liquid sodium) [1], much remained unknown concerning the nature of the electrolyte/polysulfide melt interface and the degradation of the electrolyte in contact with positive electrode (sulfur/ sodium polysulfide melts). In the present paper, the interfacial reactions between the solid electrolyte and the melts, with or without participation of impurities, were postulated from thermodynamic calculations and compared to experimental observations.

2. Experimental

2.1. Materials

(1) Polysulfides: Four different polysulfides, Na_2S_2 , Na_2S_3 , Na_2S_4 , and Na_2S_5 , and pure sulfur were used. The pure sulfur was obtained from the Lawrence Livermore Laboratory.* The disulfide Na_2S_2 was prepared from the monosulfide Na_2S (from NOAH Chemicals) and from pure sulfur in our laboratory, in a dry-box (oxygen and water free to less than 1 ppm). After the pure sulfur was dried in the dry-box for 3 days, the appropriate amount of Na_2S and dry sulfur powders were mixed and put in a quartz tube, sealed at about 10^{-2} Torr, and then slowly heated to $750^{o}C$ to form Na_2S_2 . The Na_2S_2 was cooled to room temperature and transferred to glass test tubes within the dry box. The Na_2S_3 was obtained from Brown-Boveri and Cie (BBC) and stored in vacuum. The Na_2S_4 was prepared by Dow Chemicals Co. and stored in the dry box. Na_2S_5 was made from mixtures of either Na_2S_3 or Na_2S_4 with pure sulfur.

(2) β "-Alumina Electrolyte: The polycrystalline electrolyte consisted of bars with approximate dimensions of 45x10x4mm, and was prepared by Ceramatec of Salt City, Utah [2]. The chemical composition given by the manufacturer was 8.85 wt% Na_2O 0.7 wt% Li_2O, balance Al_2O_3 .

2.2. Specimen Preparation

Two different surfaces - polished and as-sintered - were examined to determine how the surface morphology affects the stability of the electrolyte. Specimens were sectioned with a diamond saw, ground with $\alpha - Al_2O_3$ and polished to an 1 micron diamond finish (Fig 1a). Even though the polished surfaces were very smooth, some imperfections, such as cavities and large grains still remained. Mechanical damage, including microcracks, may also be produced during polishing. As-sintered surfaces are shown in Fig 2a. Some workers have reported that these surfaces might be covered by a thin, glassy film, which would be formed during sintering [3]. Specimens having different surface morphologies were washed with methyl alcohol in an ultrasonic cleaner, and then heated up to $800^{o}C$ for 12 hours to drive off absorbed water.

Lawrence Livermore National Laboratory, P. O. Box 808, Livermore, California 94550.

2.3. Impurity Contamination

Water: Electrolyte specimens were either exposed to 100% relative humidity or immersed in distilled water at room temperature for one week (168 hours) to pick up water. Then, the surface water was removed by heating the specimens at $100^{o}C$ for 5 minutes.

Oxygen: After vacuum-drying and before sealing, oxygen gas was put into the test tubes to build up an oxygen atmosphere of about 100 Torr.

Moist Air: The dried electrolyte was exposed to atmosphere (moist air) at room temperature for 1 week (168 hours).

Fe-Ni-Cr and C: Cell container materials (stainless steel) and current collector material (graphite felt) were put in with some polysulfide powders, before sealing the glass capsules.

2.4. Procedures

Because of the sensitivity of polysulfides to moisture, the test must be set up in a water and oxygen free glove box. Specimens and polysulfides were put into glass test tubes in the dry box and sealed under mechanical vacuum. The sealed tubes were placed vertically in a box furnace at the desired temperatures ($350^{o}C$ or $400^{o}C$). After the specimens had been kept in molten polysulfides for the desired period (5 weeks or 10 weeks), the glass tubes were cooled to room temperature and broken. The specimens were removed, ultrasonically cleaned in methyl alcohol, and dried, before characterization and analysis. Specimens immersed in sulfur were cleaned in CS_2 .

3. Results

3.1. Morphological Characterization

1. Effect of Composition

Figs 1 and 2 show the changes in surface morphology of electrolytes before and after 5-week immersion in melts with compositions of Na_2S_3 , Na_2S_4 , and Na_2S_5 , at $400^{o}C$, and Na_2S_2 and pure sulfur at $350^{o}C$.

The surfaces of polished specimens are shown in Fig 1. Very little has happened to the polished surface immersed in Na_2S_2 and Na_2S_3 melts. However, on the polished surface in Na_2S_4 melt, some compounds formed on areas containing defects such as microcracks, pores,

etc, which were introduced by mechanical polishing. On the polished surface immersed in Na_2S_5 , a non-uniform and discontinuous, thin surface layer was formed and more corrosion products were evident at areas containing flaws or irregularities (Fig 1e). The changes in surface morphology were even more pronounced for the samples immersed in pure sulfur, where a thick corrosion layer formed on the whole surface (Fig 1f).

The surfaces of sintered electrolyte are shown in Fig 2. After immersion, the surfaces were covered with a thin product layer, while some compounds had accumulated in the surface pores. The extent of the reactions apparently increased from Na_2S_2 to Na_2S_5 to pure sulfur.

2. Effect of Impurity Contamination

Figs 3 and 4 show the changes in morphology of polished and sintered surfaces before and after immersion at 400^oC for 5 weeks in Na_2S_3 with the presence of oxygen, water, moist air, or stainless steel (Fe-Ni-Cr) plus graphite felt (C). An Na_2S_3 melt was chosen because, without impurities, this melt was among the least reactive ones, as shown in Figs 3b and 4b. However, in the presence of impurities, the change in surface morphology and chemistry can be dramatic.

(1). Steel + Carbon (Figs 3c and 4c): The presence of transition metals and graphite felt considerably affected the interaction between the Na_2S_3 melt and the electrolyte. A corrosion product layer covered the entirety of the surface, and some octahedrally shaped crystals had formed.

(2). Oxygen (Figs 3d and 4d): The effects of the presence of oxygen contamination on the Na_2S_3/electrolyte system are: (i) creation of a corrosion layer on most of the areas of the polished surfaces (Fig 3d); (ii) considerable acceleration of the reactions and increase of the deposition of the corrosion products, and formation of the flower-shaped crystals on the electrolyte surface; and (iii) recrystallization of some crystals on the sintered surface in addition to the overall thin product layer that formed without oxygen present.

(3). Water (Figs 3e and 4e): In the case of absorption of water in electrolytes, there is an obvious etching effect: the grain boundaries are clearly revealed and some material appeared missing. Some corrosion products had deposited between grains.

(4). Moist Air (Figs 3f and 4f): The exposure of the electrolyte to moist air (H_2O , O_2 , CO_2 , etc) had the combined effects of water and oxygen contamination.

3. Time Dependence

Figs 5 and 6 show the changes in surface morphology of electrolytes before and after immersion for 5 and 10 weeks in molten Na_2S_5 , at 400^oC. Na_2S_5 was chosen in this case because this composition has the strongest corrosive effect, and hence would make differences most obvious as immersion time increased, if the corrosion were time dependent.

(1). Polished Electrolytes (Fig 5).

Fig 5a shows the surface of an as-polished electrolyte before immersion. 5 weeks later, some corrosion compounds are non-uniformly distributed, most of them concentrated around imperfections (Fig 5b). After 10 weeks, a uniform compound layer, covering the whole surface, had formed and some recrystallization had occurred, leading to the groups of plate-shaped crystallites (Fig 5c). The high-magnification micrograph (d) shows that the layer is porous but not entirely uniform: more corrosion products had accumulated in defect areas.

(2). Sintered Electrolytes (Fig 6).

A comparison with virgin materials clearly indicates that a compound layer, covering the entire surface, was well established after 5 weeks immersion with some crystals just starting to grow (Fig 6b). However, many more new crystals and compounds, formed at grain junctions, were found on the surface after 10 weeks immersion (Figs 6c and d). An even higher magnification micrograph (e) shows the detailed morphology of the flower-shaped crystal clusters and the thin layer. The thin layer looks porous and developed deeper in the defected areas where corrosion product recrystallization apparently had occurred.

3.2. Chemical Characterization

An Auger electron spectrum obtained from a polished surface of samples immersed in the Na_2S_5 melt for 10 weeks is shown in Fig 7a. The elements present in the spectrum should represent the average composition of corrosion compounds. Fig 7b shows the profile of the impurities in the degraded layer at different sputtering time. The quantity of sulfur decreases as sputtering time increases, clearly indicating that a reaction or corrosion layer had formed on electrolyte surface. This layer was sputtered off in 10 mins. The sulfur probably was present as sulfates because a large quantity of oxygen was also detected at the same time. Attempts to identify the corrosion compounds by X-ray diffraction were unsuccessful.

4. Discussion

Experimental observations indicated that the electrolyte reacts chemically with Na_2S_x melts. To identify possible reactions at the electrolyte/melt interface, thermodynamic calculations were performed.

4.1. Thermodynamic Considerations

The Gibbs free energies of formation of sodium polysulfides, tabulated in Table 1, were calculated by Gupta [4] from open circuit cell voltage measurements. The only data on the Gibbs free energy of formation of a solid electrolyte with composition $Na_2O{\cdot}8Al_2O_3$, are those obtained by Weber with electrochemical methods and calculated by Kummer [5]. These data were evaluated for temperatures between 1027^oC and 1627^oC , and have to be extrapolated to temperatures around $350—400^oC$. They have been tabulated in Table 1. Other data are from the NBS tables of chemical thermodynamic properties [6] and JANAF thermochemical tables [7]. Some values for 350^oC and 400^oC were calculated from the data at 25^oC.

The reactions involving the liberation of free Al_2O_3 should probably consider the formation of metastable Al_2O_3 phases rather than $\alpha—Al_2O_3$ phase. However, we have to assume that the reactions considered here will produce $\alpha—Al_2O_3$ because neither free energy nor structural data are available for the metastable Al_2O_3 decomposition products.

Based on these thermodynamic data and assumptions, the standard Gibbs free energies for the reactions between the solid electrolyte and sodium polysulfide melts are calculated as follows:

$$\Delta_r G^o = \sum_i (\nu_i \cdot \Delta_f G^o)_{(product)} - \sum_i (\nu_i \cdot \Delta_f G^o)_{(reactant)} \qquad (4.0)$$

The chemical reactions that could occur on the surfaces of the electrolytes are postulated as follows:

(1). Reactions Between **Pure Sulfur** and β "Alumina

$$Na_2O{\cdot}8Al_2O_3 + \frac{(3x+1)}{4}S \rightarrow \frac{3}{4}Na_2S_x + \frac{1}{4}\mathbf{Na_2SO_4} + 8Al_2O_3 \qquad (4.1a)$$

$$Na_2O{\cdot}8Al_2O_3 + \frac{(3x+1)}{3}S \rightarrow Na_2S_x + \frac{1}{9}\mathbf{Al_2(SO_4)_3} + 7\frac{8}{9}Al_2O_3 \qquad (4.1b)$$

$$Na_2O{\cdot}8Al_2O_3 + \frac{(12x+4)}{13}S \rightarrow \frac{2}{13}\,\mathbf{NaAl(SO_4)_2} + \frac{12}{13}Na_2S_x + 7\frac{12}{13}Al_2O_3 \qquad (4.1c)$$

(2) Reactions Between $\mathbf{Na_2S_x}$ and β " Alumina

$$Na_2O{\cdot}8Al_2O_3 + \frac{(3x-2)}{4}Na_2S_x \rightarrow \frac{1}{4}\mathbf{Na_2SO_4} + \frac{(3x+1)}{4}Na_2S_{(x-1)} + 8Al_2O_3 \quad (4.2a)$$

$$Na_2O{\cdot}8Al_2O_3 + \frac{(3x-2)}{3}Na_2S_x \rightarrow \frac{1}{9}\ \mathbf{Al_2(SO_4)_3}\ + \frac{(3x+1)}{3}Na_2S_{(x-1)} + 7\frac{8}{9}Al_2O_3, \quad (4.2b)$$

$$Na_2O{\cdot}8Al_2O_3 + \frac{4(3x-2)}{13}Na_2S_x \rightarrow \frac{2}{13}\mathbf{NaAl(SO_4)_2} + \frac{4(3x+1)}{13}Na_2S_{(x-1)} + 7\frac{12}{13}Al_2O_3 \quad (4.2c)$$

The reactions with negative Gibbs free energies, see Table 2, are the ones thermodynamically possible, although some may not be fast enough to be significant.

The reaction mechanism could involve at first a partial Na^+ depletion of the electrolyte, described by

$$Na^{X}_{N_a}(E) = Na^{+}(M) + V'_{Na}(E) \quad (4.3a)$$

Where E and M refer to the solid electrolyte and to the melt, respectively.

$$Na^{X}_{N_a}(E) + e' + \frac{(x-1)}{2}Na_2S_x(M) \rightarrow \frac{x}{2}Na_2S_{(x-1)}(M) + \mathbf{V'_{Na}}(E) \quad (4.3b)$$

or

$$Na^{X}_{N_a}(E) + e' + \frac{x}{2}S(M) \rightarrow \frac{1}{2}Na_2S_x(M) + \mathbf{V'_{Na}}(E)$$

Electro-neutrality requires that the crystal release the excess oxygen (Eq 4.3c). This oxygen can react with Na_2S_x (M) to give SO_3 (Eq 4.3d).

$$O^{X}_{O}(E) \rightarrow \ddot{V}_O(E) + \frac{1}{2}\mathbf{O_2}(M) + 2e' \quad (4.3c)$$

$$O_2(M) + \frac{2}{3}Na_2S_x(M) \rightarrow \frac{2}{3}Na_2S_{(x-1)}(M) + \frac{2}{3}\mathbf{SO_3}(M) \quad (4.3d)$$

The SO_3 can react further to produce corrosion products: sulfates- Na_2SO_4 , $NaAl(SO_4)_2$, $Al_2(SO_4)_3$, etc, through the reactions:

$$SO_3 + Na_2O{\cdot}8Al_2O_3 \rightarrow \mathbf{Na_2SO_4} + 8Al_2O_3 \quad (4.3e)$$

$$SO_3 + \frac{1}{4}Na_2O{\cdot}8Al_2O_3 \rightarrow \frac{1}{2}\ \mathbf{NaAl(SO_4)_2}\ + \frac{7}{4}Al_2O_3$$

$$SO_3 + \frac{1}{25}Na_2O{\cdot}8Al_2O_3 \rightarrow \frac{8}{25}\ \mathbf{Al_2(SO_4)_3}\ + \frac{1}{25}Na_2SO_4$$

The combination of these reactions gives the over-all equations 4.2a, b, and c.

In brief, then, (1) chemical reactions initiate at surface imperfections, and (2) since the degraded layer is porous, the reaction will continue to develop into the β " alumina, preferentially on these areas of imperfections.

β " alumina electrolytes, used in the as-sintered state, may be covered by a very thin, soda-rich, glassy surface film [3]. Such a film would not be as stable as the crystalline electrolyte. Therefore, the reactions 4.1 and 4.2, are expected to be more favorable initially on the sintered surface compared to the polished surface from which such film have been removed.

Both experimental observations and thermodynamic calculations, summarized in Table 2, indicate that the corrosion power of sodium polysulfide melts increases as the content of sulfur increases from Na_2S_2 to Na_2S_5, the normal composition range of a practical cell operation.

4.2. Influence of Impurity Contamination

1. Oxygen

With the participation of oxygen, the chemical reactions can be written as follows:

$$\mathbf{O_2} + \frac{2(x-1)}{(3x+1)}Na_2O{\cdot}8Al_2O_3 + \frac{2}{(3x+1)}Na_2S_x \rightarrow \frac{2x}{(3x+1)}\mathbf{Na_2SO_4} + \frac{16(x-1)}{(3x+1)}Al_2O_3 \qquad (4.4a)$$

$$\mathbf{O_2} + \frac{(x-1)}{2(3x+1)}Na_2O{\cdot}8Al_2O_3 + \frac{2}{(3x+1)}Na_2S_x \rightarrow \frac{(x-1)}{(3x+1)}\mathbf{NaAl(SO_4)_2} + \frac{2}{(3x+1)}\mathbf{Na_2SO_4} + \frac{7(x-1)}{2(3x+1)}Al_2O_3 \qquad (4.4b)$$

$$\mathbf{O_2} + \frac{[96+(3x-2)(x-1)]}{48(3x+1)}Na_2S_x + \frac{(x-1)}{12(3x+1)}Na_2O{\cdot}8Al_2O_3 \rightarrow \frac{2(x-1)}{3(3x+1)}\mathbf{Al_2(SO_4)_3} + \frac{(x-1)}{48}Na_2S_{(x-1)} + \frac{[96+(x-1)]}{48(3x+1)}\mathbf{Na_2SO_4} \qquad (4.4c)$$

Obviously, these reactions are much more favorable thermodynamically in the presence of oxygen, since they have a large, negative $\Delta_r G^o$, as shown in Table 3. Experimental results agreed very well with this calculation. A heavy reaction, deposition of corrosion products, and recrystallization were found on the electrolyte surfaces when some free oxygen had been introduced into test tubes before sealing (see Figs 3d and 4d).

2. Water

When water has intercalated in the electrolyte, the reactions between β'' alumina and polysulfides changed and the corrosion products expected here were $NaHSO_4$ and Na(OH), which could cause continued dissolution of the electrolyte.

$$\mathbf{Na_2O{\cdot}8Al_2O_3} + \frac{x(3x-2)}{(4x-1)}Na_2S_x + \frac{(x-1)}{(4x-1)}H_2O \rightarrow \frac{(3x+1)x}{(4x-1)}Na_2S_{(x-1)} + \frac{x}{(4x-1)}\mathbf{NaHSO_4} + \frac{(x-2)}{(4x-1)}\mathbf{NaOH} + 8Al_2O_3 \quad (4.5a)$$

If water and oxygen coexist, the reaction should be:

$$H_2O + \frac{(x-2)}{(x-1)}Na_2O{\cdot}8Al_2O_3 + \frac{1}{(x-1)}Na_2S_x + \frac{(3x+1)(x-2)}{(x-1)(2x-4)}\mathbf{O_2} \rightarrow \frac{x}{(x-1)}\mathbf{NaHSO_4} + \frac{(x-2)}{(x-1)}\mathbf{NaOH} + \frac{8(x-2)}{(x-1)}Al_2O_3 \quad (4.5b)$$

The additional presence of oxygen makes the reactions possible, as it is evident in Table 3.

3. Moist Air

If some O_2 , CO_2 , and H_2O are present by absorption from moist air, which is almost unavoidable, the following initial reactions are quite favorable, as follows from an examination of their $\Delta_r G^o$ values listed in Table 3.

$$Na_2S_x + H_2O + CO_2 + \frac{3(x-1)}{2}O_2 \rightarrow \mathbf{Na_2CO_3} + H_2S + (x-1)SO_3 \quad (4.6a)$$

The H_2S and SO_3 react further with the electrolyte to form sulfates: $NaHSO_4$, $Al_2(SO_4)_3$, $NaAl(SO_4)_2$, etc.

$$Na_2S_x + Na_2O{\cdot}8Al_2O_3 + \frac{(3x+1)}{2}\mathbf{O_2} + H_2O + CO_2 \rightarrow \mathbf{Na_2CO_3} + 2\mathbf{NaHSO_4} + \frac{(26-x)}{3}Al_2O_3 + \frac{(x-2)}{3}\mathbf{Al_2(SO_4)_3} \quad (4.6b)$$

$$Na_2O{\cdot}8Al_2O_3 + \frac{2(3x+1)}{(x+2)}\mathbf{O_2} + \frac{4}{(x+2)}[Na_2S_x + H_2O + CO_2] \rightarrow \frac{4}{(x+2)}\mathbf{Na_2CO_3} + \frac{8}{(x+2)}\mathbf{NaHSO_4} + \frac{(7x+18)}{(x+2)}Al_2O_3 + 2\frac{(x-2)}{(x+2)}\mathbf{NaAl(SO_4)_2} \quad (4.6c)$$

$$Na_2O{\cdot}8Al_2O_3 + \frac{(3x+1)}{2(x-1)}\mathbf{O_2} + \frac{1}{(x-1)}[Na_2S_x + H_2O + CO_2] \rightarrow \frac{1}{(x-1)}\mathbf{Na_2CO_3} + \frac{2}{(x-1)}\mathbf{NaHSO_4} + \frac{(x-2)}{(x-1)}\mathbf{Na_2SO_4} + 8Al_2O_3 \quad (4.6d)$$

Coupled with oxygen or even carbon dioxide, which could come from the absorption of moist air on the electrolyte surface during cell construction, water does make the polysulfides more susceptible to corrosion. The possible reaction products now include $NaHSO_4$ and Na(OH), whose melting points are 320^oC and 317^oC, respectively. Thus, the presence of water can lead to increased reaction of the electrolyte in the polysulfide melts at about 350^oC (see Figs 3e and 4e).

4. Fe-Ni-Cr and C

An important aspect of sulfur side-degradation in practical Na/S cells is deposition of metal sulfides originating from container corrosion. The deposits formed on the electrolyte surface, as shown in Figs 3c and 4c, have been identified as FeS_2 , Cr_2S_3 , Ni_3S_2 , NiS_2, (Ni,Fe)S and $NaCrS_2$, etc., and are similar to those reported by Park [8] and Battles [9]. The possible reactions can be written as follows:

$$Fe + 2Na_2S_x \rightarrow 2Na_2S_{(x-1)} + \mathbf{FeS_2} \tag{4.7a}$$

$$7Fe + 8Na_2S_x \rightarrow 8Na_2S_{(x-1)} + \mathbf{Fe_7S_8}$$

$$3FeS_2 + 4SO_3 + 7Na_2S_x \rightarrow \mathbf{3FeSO_4} + 7Na_2S_{(x+1)}$$

$$Ni + Na_2S_x \rightarrow Na_2S_{(x-1)} + \mathbf{NiS} \tag{4.7b}$$

$$3Ni + 2Na_2S_x \rightarrow 2Na_2S_{(x-1)} + \mathbf{Ni_3S_2}$$

$$2Cr + 3Na_2S_x \rightarrow 3Na_2S_{(x-1)} + \mathbf{Cr_2S_3} \tag{4.7c}$$

$$3Cr + 2C \rightarrow \mathbf{Cr_3C_2}$$

$$7Cr + 3C \rightarrow \mathbf{Cr_7C_3}$$

The reactions between the electrolyte and carbon have also been studied recently by Choudhury [10]. The proposed reaction products include Na_2CO_3 and CO.

4.3. Dissolution/Recrystallization

As shown in Figs 5 and 6, after 5 weeks immersion, the sulfates produced by the reactions described above, had not yet saturated the Na_2S_x melts, and not much recrystallization was found at that time. After 10 weeks immersion, however, the melts were saturated with the

sulfates, and a lot of recrystalization was found on all the surfaces of the electrolyte. The recrystallized, flower-like, crystals, as clearly seen in Fig 6, are believed to be sodium sulfates.

It appears, see Fig 1 and 2, that more chemical reactions, deposition and or recrystallization of corrosion products occurred in sulfur-rich melts, i.e., Na_2S_5 and pure sulfur, and that more dissolution of corrosion products occurred in sulfur-poor melt, i.e., Na_2S_2. This is perhaps due to the changes of the solubility of the sulfates in the sulfide melts as the composition of the sulfides changes.

5. Conclusions

Sodium β'' alumina electrolytes are chemically attacked by Na_2S_x melts and pure sulfur during immersion at high temperatures. The likely reactions can be written as described in Eqs 4.1 though Eq 4.7, and occur preferentially on surface imperfections of the solid electrolyte.

The corrosion products are believed to be sulfates: Na_2SO_4 , $NaAl(SO_4)_2$, $Al_2(SO_4)_3$, $NaHSO_4$, Na_2CO_3 and NaOH. Most of these have high melting point and deposit on the electrolyte surface. Some have a low melting point and can be dissolved in the polysulfide melts, leading to dissolution or etching of the electrolyte surface.

There is a limited solubility of sodium sulfates in sodium sulfide melts. Recrystallization of the sulfate occurred after prolonged exposure to sulfide melts and occurred preferentially at imperfections such as boundaries of large grains, or surface steps on the electrolyte surface.

The degree of corrosion increased as the content of sulfur increases in the range of Na_2S_2 to Na_2S_5 to sulfur.

In addition to the reactions between β'' alumina and Na_2S_x or sulfur, the corrosion products of transition metals, and current collector material (graphite), also deposit on the electrolyte surface.

All of the corrosion reactions were greatly accelerated by contaminations of impurities, such as water and oxygen, and transition metals.

In a practical cell, the environment the electrolyte will be exposed to is a combination of the above situations. The degraded layer formed on electrolyte surfaces in a real cell is expected to be a mixture of (1) sulfates and carbonates, produced by reactions 4.1 through 4.6, and (2) corrosion products of cell parts, by reactions 4.7. Since the corrosive power of the

polysulfide melts increases at composition corresponding to the full charged state and is enhanced by free sulfur, it would seem advisable to avoid heterogeneous electrode reactions that expose the electrolyte surface for unnecessarily long periods to the most corrosive sulfide melts.

Acknowledgements

The authors wish to thank Dr. S. Visco for valuable discussions and suggestions .

This work was supported by the U. S. Department of Energy under contract No. DE-AC03-76SF00098.

References

[1] De Jonghe, L. C., L. Feldman, and A. Buechele, Solid state Ionics, 5 (1981) 267-270.

[2] Miller, M. L., B. J. McEntier, G. R. Miller and R. S. Gordon, Amer. Ceram. Soc. Bull., Vol.58, No.5 (1979) 522-6.

[3] Singh, R. N., J. Am. Ceram. Soc., Vol.67, No.10 (1984) 637.

[4] Gupta, N. K., and Tischer, R. P., J. Electrochem. Soc., 119, 1033 (1972).

[5] Kummer, J. T., Progress in Solid State Chemistry Vol.7, p. 141-175, ed. by H. Reiss and J. O. McCaldin, Pergamon Press, N. Y., 1972.

[6] The NBS Tables of Chemical Thermodynamic Properties, J. Phys. and Chemical Ref. Data, Vol.11, Supplement No.2, 1982.

[7] JANAF Thermochemical Tables, 2ed ed., Nat. Stand. Ref. Data Ser., Nat. Bur. Stand. (U.S.), 37, 1971, 1978; J. Phys. and Chem. Ref. Data, Vol.11, No.3, 1982.

[8] Park, Dong-sil, Proceeding: DOE/EPRI Beta (Sodium-Sulfur) Battery Workshop V, EPRI EM-3631-SR, (1984) PP6-191.

[9] Battles, J. E., Proceeding: DOE/EPRI Beta (Sodium-Sulfur) Battery Workshop V, EPRI EM-3631-SR, (1984) PP6-291.

[10] Choudhury, N. S., J. Electrochem. Sco., Vol. 133, No.2 (1986)425-431

Tables

Table 1

The standard Gibbs free energies of formation of sodium polysulfides, α-alumina, sodium oxide and β "-alumina [KJ/mol.]				
Compound	$300^{o}C$	$350^{o}C$	$400^{o}C$	Source
Na_2S_5	- 401.8	- 400.8	- 400.6	Gupta
Na_2S_4	- 398.9	- 398.1	- 398.1	
Na_2S_3	- 398.7	- 388.2	- 386.0	
Na_2S_2	- 375.1	- 370.0	- 365.0	
Na_2S	- 338.1	- 335.7	- 333.2	JANAF
α-Al_2O_3	-1496.5	- 1480.9	-1465.2	
Na_2O (s)	- 340.4	- 333.3	- 326.2	
Na_2O (l)	- 307.7	- 302.5	- 297.2	
β "-Al_2O_3	-12,608.7	-12,467.0	-12,325.3	Kummer

Table 2

The standard free energies of reactions between β''-alumina and sulfur/Na_2S_x (M) (without impurity contamination) [KJ/mol.]			
Equation#	x (as in Na_2S_x)	$(\Delta_r G^o)_{400C}$	$(\Delta_r G^o)_{350C}$
Eq (4.1a)	5	- 55.5	- 36.6
	4	- 53.6	- 34.6
	3	- 44.6	- 27.2
	2	- 28.8	- 13.5
	1	- 5.0	+ 12.0
Eq (4.1b)	5	- 24.6	- 4.7
	4	- 22.1	- 2.0
	3	- 10.0	+ 7.9
	2	+ 11.0	+ 26.1
	1	+ 42.8	+ 60.4
Eq (4.1c)	5	- 37.3	- 20.9
	4	- 34.9	- 18.4
	3	- 23.8	- 9.3
	2	- 4.4	+ 7.5
	1	+ 25.1	+ 39.2
Eq (4.2a)	5	- 45.5	- 25.7
	4	- 14.3	- 2.4
	3	+ 7.9	+ 18.3
	2	+ 26.8	+ 45.9
Eq (4.2b)	5	- 11.2	+ 9.8
	4	+ 30.3	+ 40.9
	3	+ 60.0	+ 68.5
	2	+ 85.5	+106.2
Eq (4.2c)	5	- 24.9	- 7.6
	4	+ 13.4	+ 21.2
	3	+ 40.8	+ 46.6
	2	+ 64.0	+ 81.4

Table 3.

The standard free energies of reactions between β''-alumina and Na_2S_z (M) with impurity contaminations				
Equation#	x (as in Na_2S_z)	$(\Delta_r G^o)_{400C}$	$(\Delta_r G^o)_{350C}$	Unit
Eq (4.4a)	5	-458.7	-456.6	KJ/mol.O_2
	4	-456.9	-455.6	
	3	-456.1	-455.5	
	2	-456.7	-457.5	
Eq (4.4b)	5	-408.2		KJ/mol. O_2
	4	-410.4		
	3	-415.7		
	2	-428.1		
Eq (4.4c)	5	-385.5		KJ/mol.O_2
	4	-388.8		
	3	-396.6		
	2	-414.3		
Equation#	x	$(\Delta_r G^o)_{400C}$		
		KJ/mol.H_2O	KJ/mol.β''	KJ/mol.O_2
Eq (4.5a)	5	+ 91.1	+19.2	
Eq (4.5b)	5	- 752.3		- 376.2
Equation#	x	$(\Delta_r G^o)_{400C}$		
		KJ/mol.CO_2/H_2O	KJ/mol. O_2	
Eq (4.6a)	5	- 1529.0	- 254.8	
	4	- 1171.9	- 260.4	
	3	- 824.3	- 274.8	
	2	- 485.7	- 323.8	
Eq (4.6b)	5	- 3070.9	- 383.9	
	4	- 2519.7	- 387.7	
	3	- 1978.2	- 395.6	
	2	- 1445.5	- 413.0	
Eq (4.6c)	5	- 1374.1	- 400.8	
	4	- 870.0	- 401.5	
	3	- 412.8	- 412.8	
Eq (4.6d)	5	- 3515.7	- 439.5	
	4	- 2816.3	- 433.3	
	3	- 2124.6	- 425.3	
	2	- 1445.4	- 413.0	

Figure Captions

Fig 1 Scanning electron micrographs of the polished surface of the electrolyte before and after 5-week immersion in sodium polysulfide melts with different compositions.

(a) as-polished before immersion.

(b) immersed in Na_2S_2 (350^oC).

(c) in Na_2S_3 (400^oC).

(d) in Na_2S_4 (400^oC).

(e) in Na_2S_5 (400^oC).

(f) immersed in pure sulfur (350^oC).

Fig 2 Sintered surfaces of the electrolyte (same experimental conditions and arrangement as in Fig 1)

Fig 3 SEM micrographs of the polished surfaces of the electrolyte before and after 5-week immersion, at 400^oC , in Na_2S_3 melts, with or without impurity contamination.

(a) as prepared before immersion.

(b) dry, uncontaminated samples immersed in **pure** Na_2S_3 (without impurity contamination).

(c) dry samples immersed in Na_2S_3 with **stainless steel (Fe-Ni-Cr)** and **graphite felt (C).**

(d) dry samples immersed in Na_2S_3 melt with an **oxygen** atmosphere of about 100 torr.

(e) **wet** samples immersed in Na_2S_3 melt.

(f) samples exposed to **moist air** for 1-week before immersion.

Fig 4 Sintered surfaces of the electrolyte (same experimental conditions and arrangement as in Fig 3).

Fig 5 SEM micrographs of the polished surfaces of the electrolyte immersed in **pure** Na_2S_5, at 400^oC , for different periods of time.

(a) virgin material as prepared.

(b) 5-week immersion.

(c) 10-week immersion.

(d) high magnification micrograph showing the detailed surface morphology after 10-week immersion.

Fig 6 Sintered surfaces of the electrolyte (same experimental conditions and arrangement as in Fig 5).

Fig 6e high magnification micrograph of a sintered surface showing the detailed surface morphology after 10-week immersion.

Fig 7 (A) Auger electron spectrum of a polished surface of the electrolyte after 10-week immersion in pure Na_2S_5 at 400^oC . The corresponding morphology is shown in Fig 5 (c) and (d).

(B) Profile of the impurities in the degraded (corrosion) layer formed on the electrolyte surface during 10-week immersion in pure Na_2S_5 at 400^oC (concentration of impurities vs sputtering time)

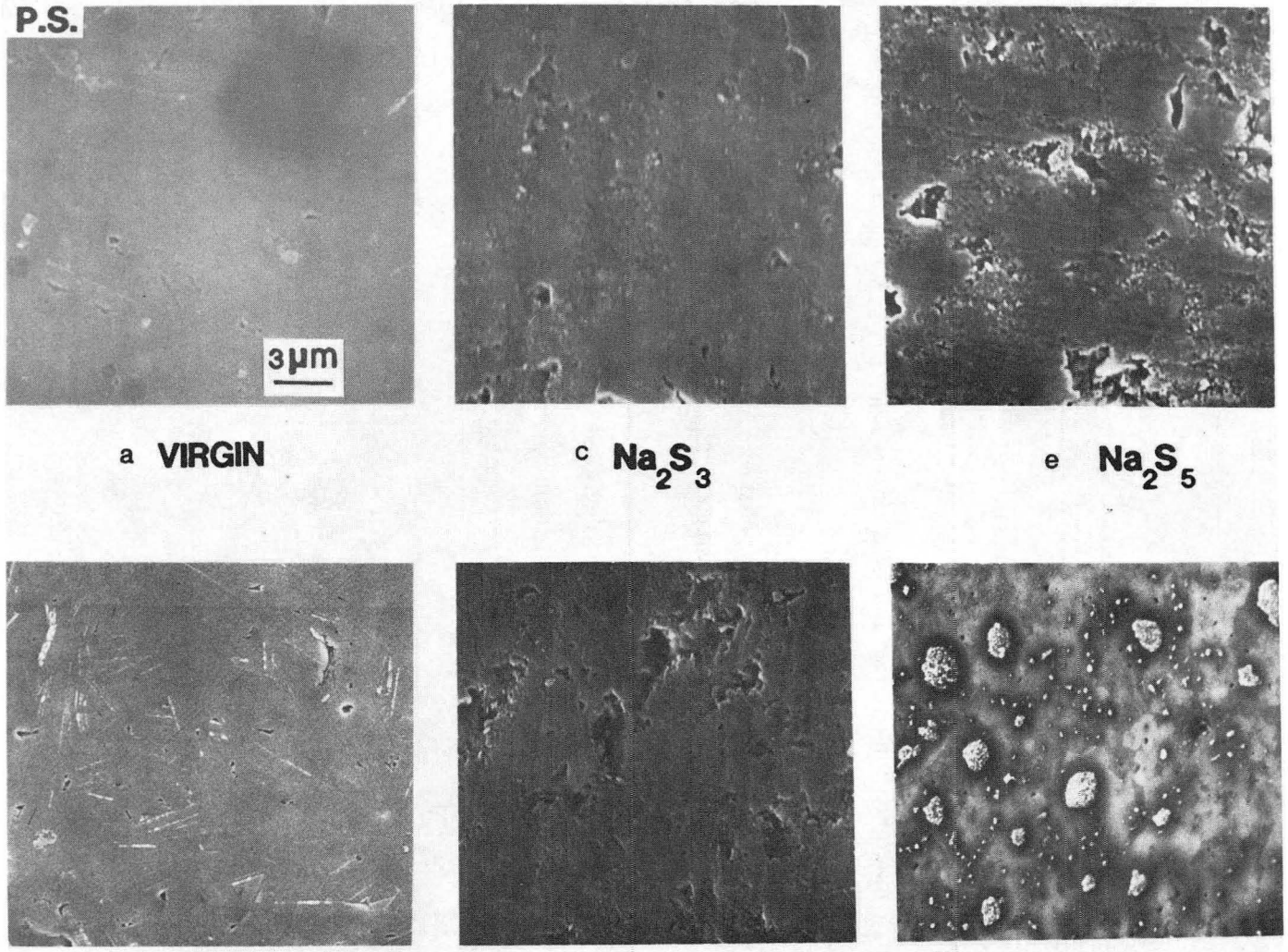

XBB 864-2699

Fig 1

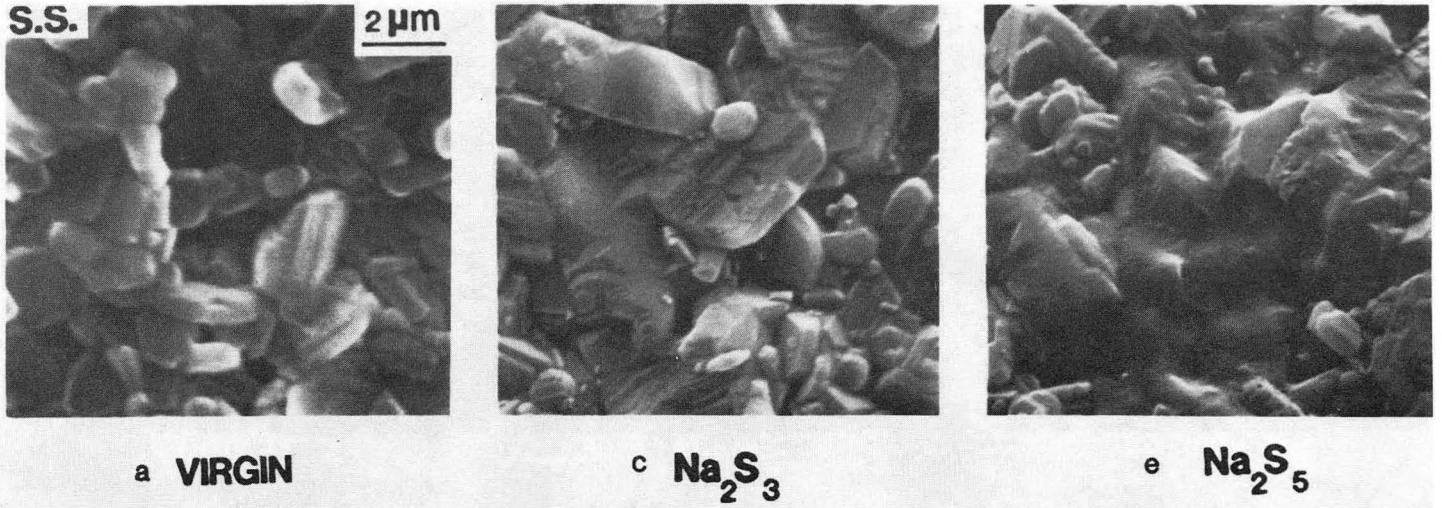

XBB 864-2698

Fig 2

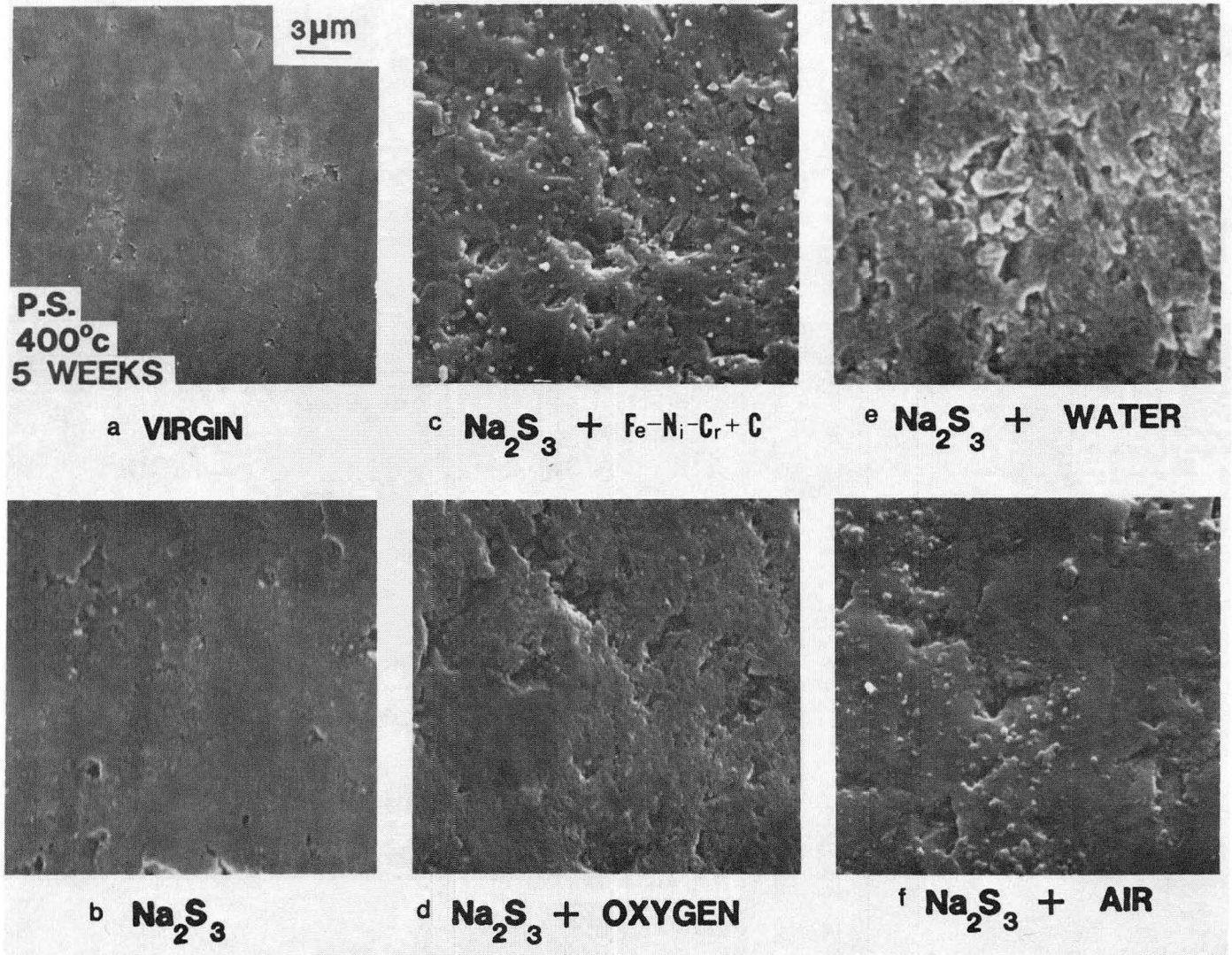

Fig 3

XBB 850-8731

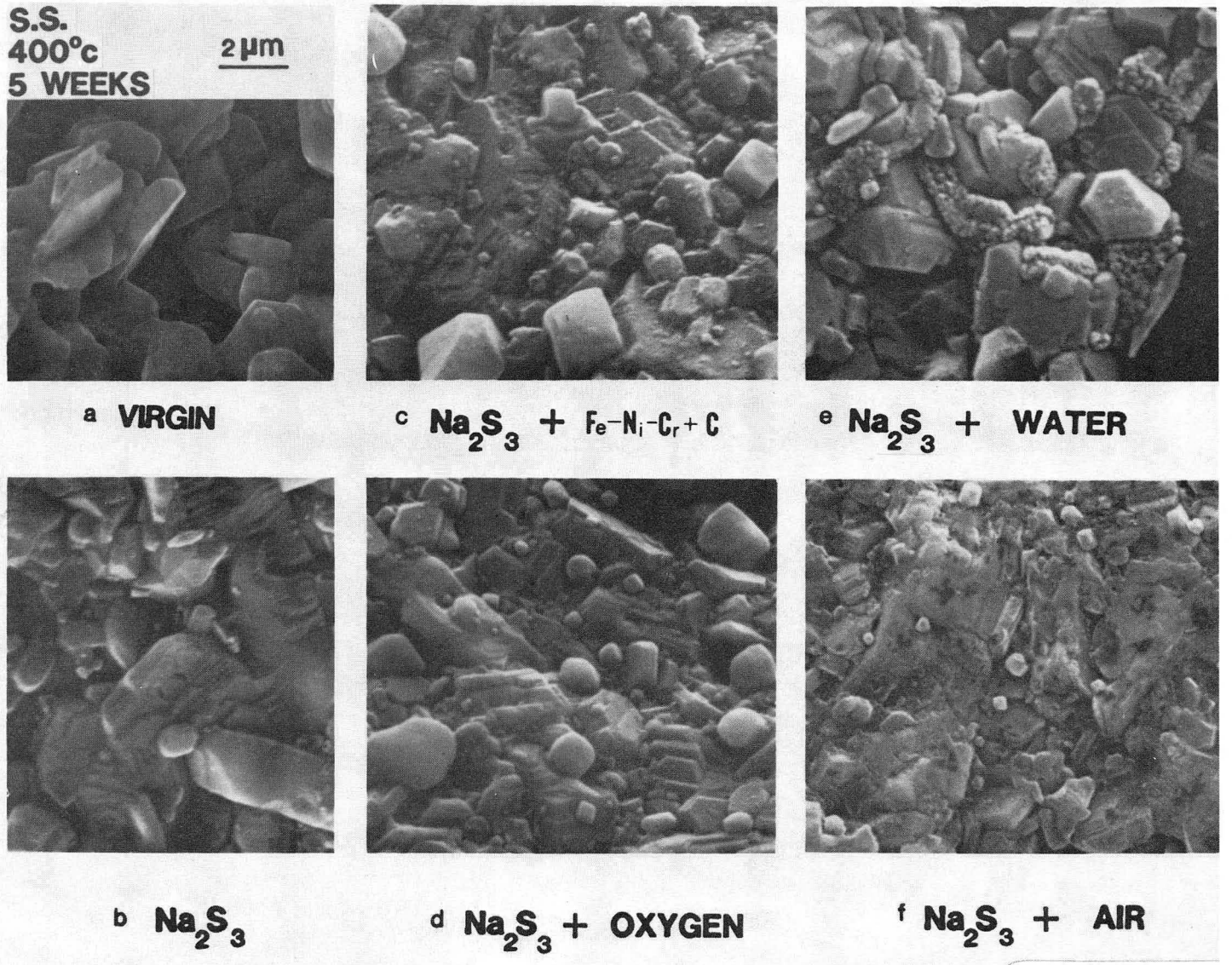

Fig 4

XBB 850-8729

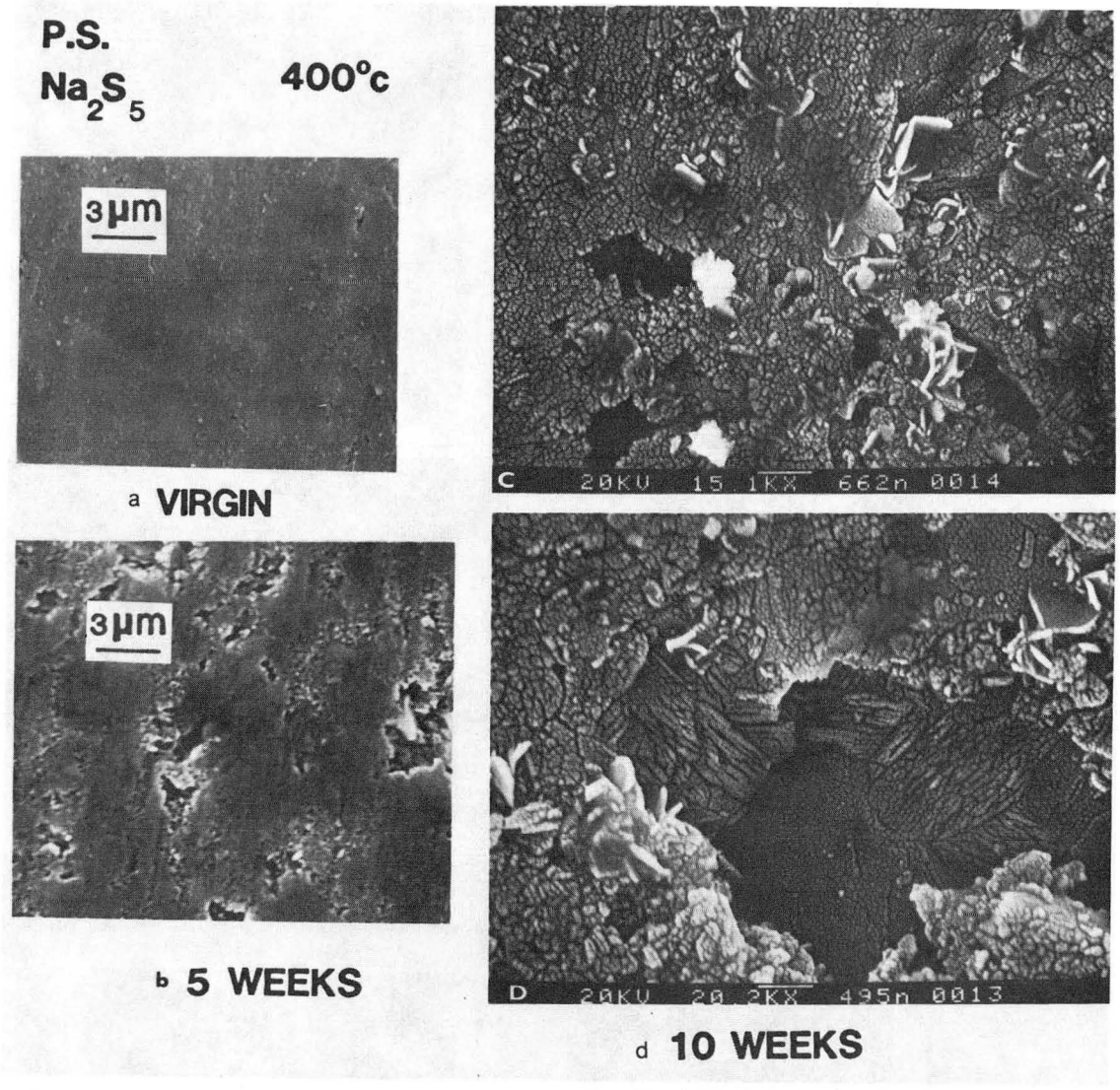

XBB 850-8969

Fig 5

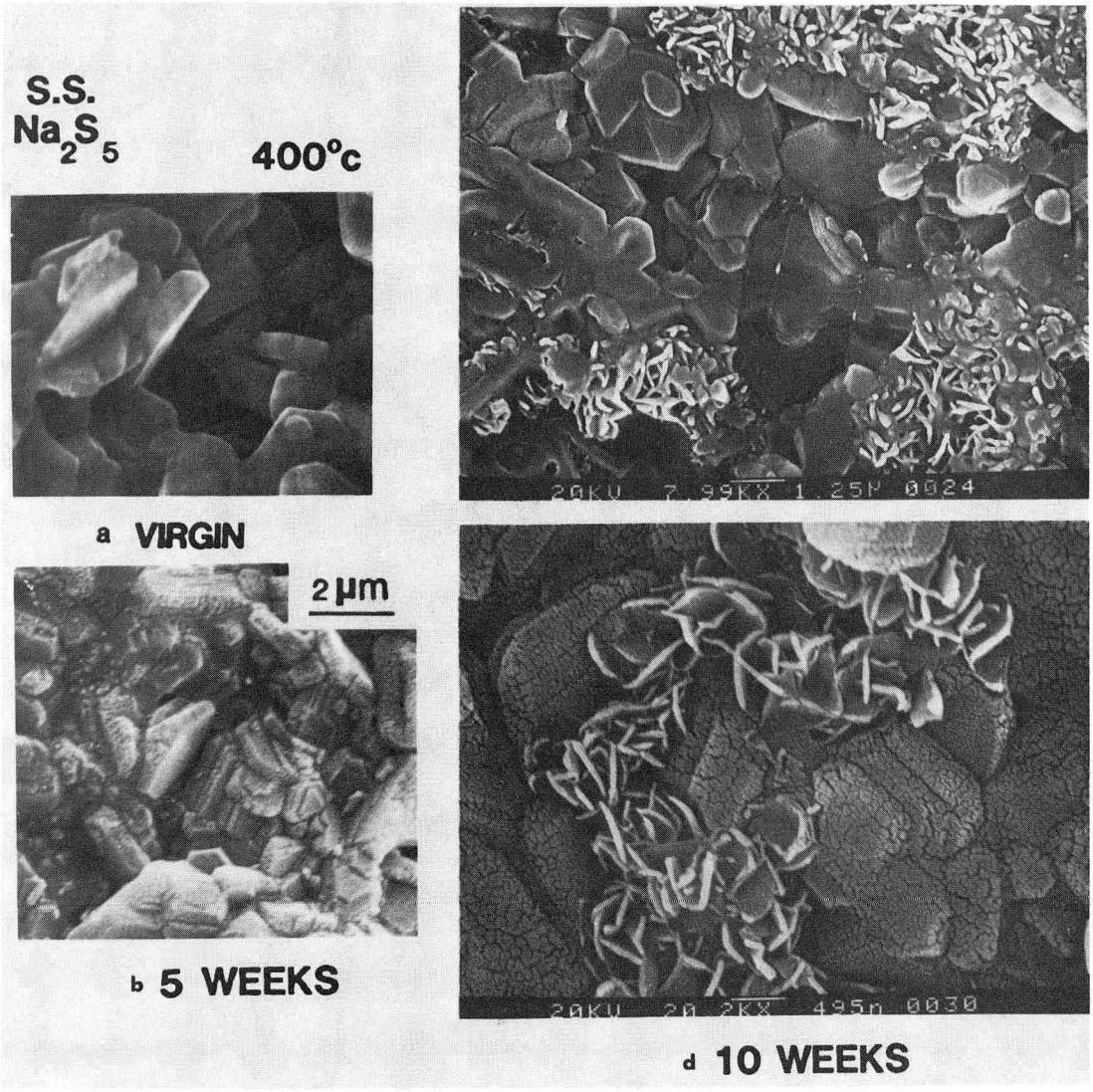

XBB 850-8967

Fig 6

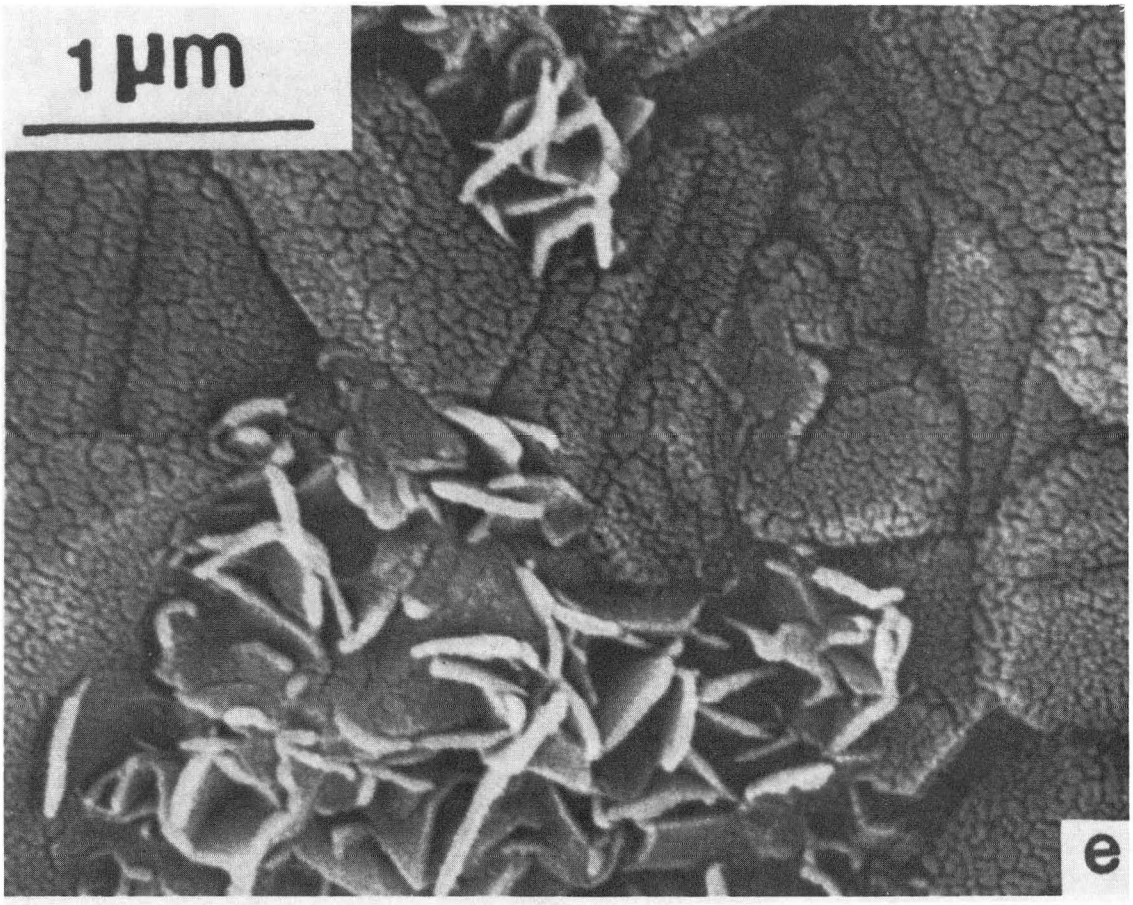

XBB 850-9044

Fig 6

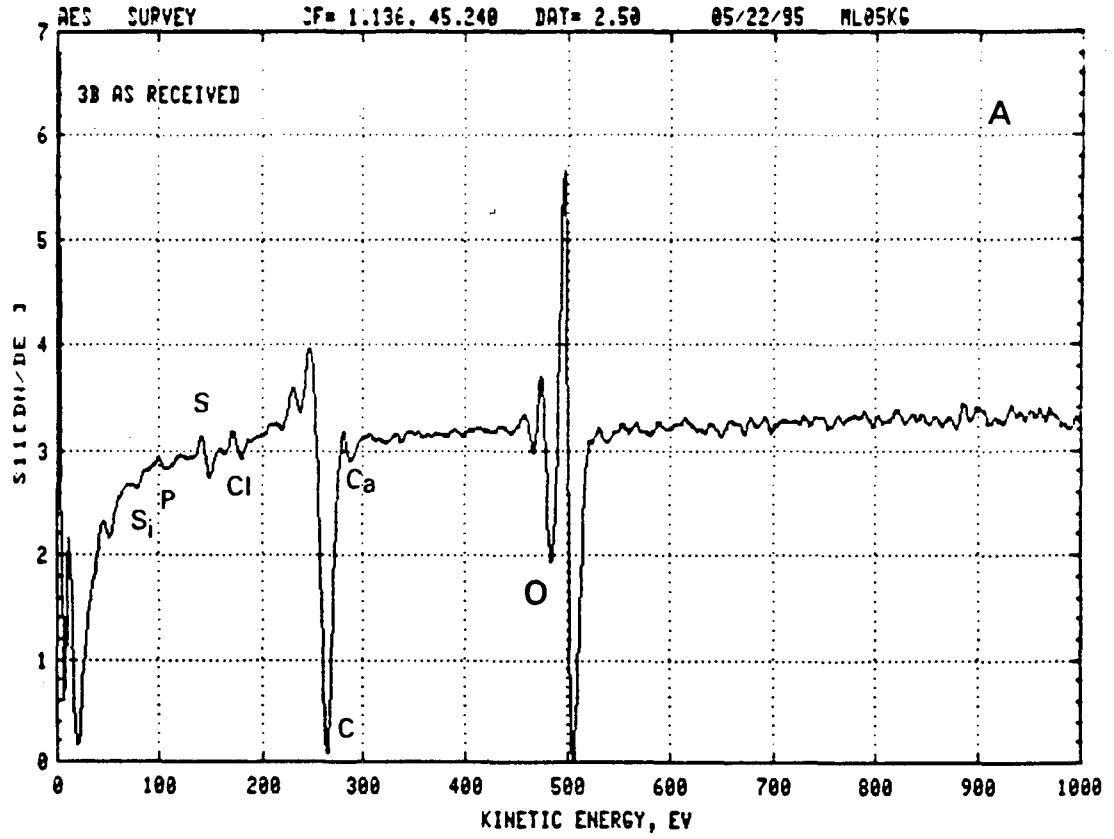
AES SURVEY CF= 1.136, 45.240 DAT= 2.50 05/22/95 ML05KG
3B AS RECEIVED
A
S
P
Cl
Si
Ca
C
O
KINETIC ENERGY, EV

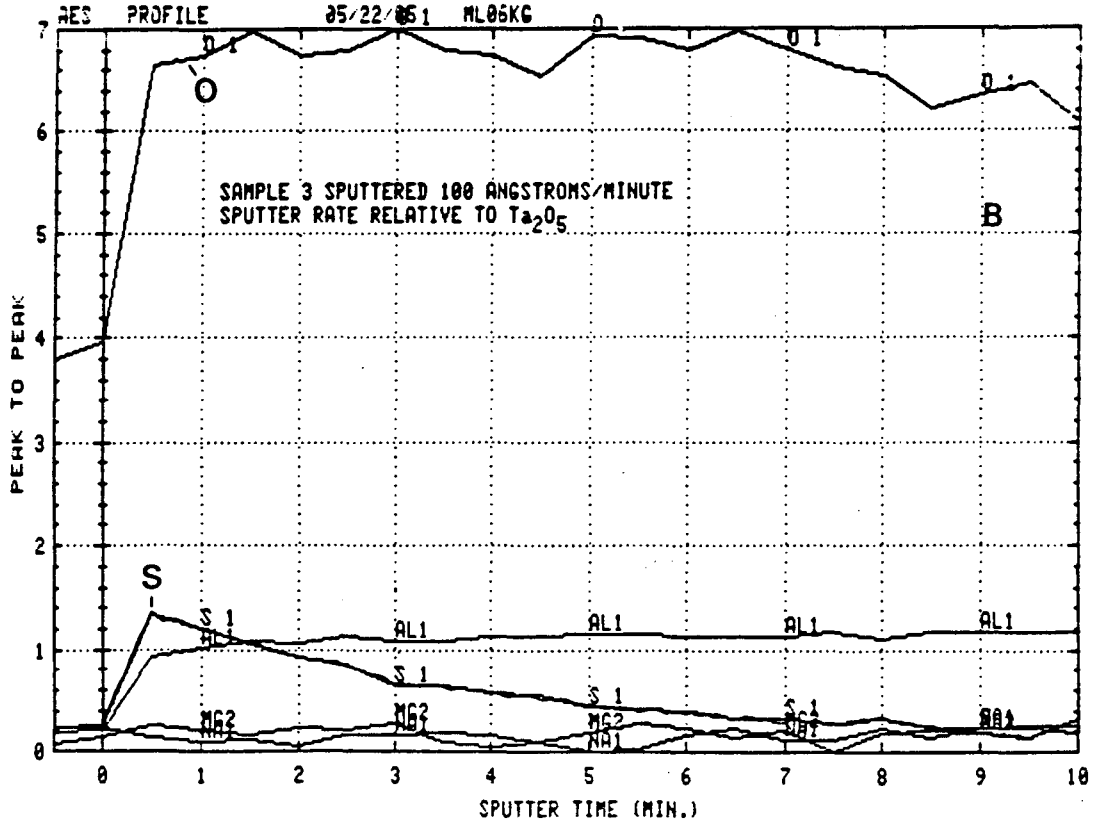
AES PROFILE 05/22/95 ML05KG
O
SAMPLE 3 SPUTTERED 100 ANGSTROMS/MINUTE
SPUTTER RATE RELATIVE TO Ta2O5
B
S
AL1
PEAK TO PEAK
SPUTTER TIME (MIN.)

Fig 7

LAWRENCE BERKELEY LABORATORY
TECHNICAL INFORMATION DEPARTMENT
UNIVERSITY OF CALIFORNIA
BERKELEY, CALIFORNIA 94720